Modeling the Logarithmic and Exponential Transformation Algorithms for Optical Density in Decision Support Models and Methods

Bohdan Durnyak[1], Mikola Lutskiv[1], Petro Shepita[1] and Inna Polishchuk[2]

[1] *Ukrainian Academy of Printing, Pid Goloskom str., 19, Lviv, 79020, Ukraine*
[2] *Uzhhorod National University, Narodna Square, 3, Uzhhorod, 88000, Ukraine*

Abstract

The problem of constructing a model for the darkness level of monochromatic halftone image printed with "black" ink based on the light reflection coefficient from the image surface using optical density in logarithmic and exponential transformation algorithms was considered. The intensity of visual perception of optical density within a specified tone reproduction range was quantitatively evaluated and analyzed. Characteristics of optical density dependence for different transformation algorithms were determined and analyzed in terms of their properties. Deviations, sensitivity to changes in parameters, and the intensity of visual perception of optical density were determined between the algorithms.

For modeling and studying the transformation algorithms, the MATLAB package, specifically Simulink, was applied. Based on this, a structural model scheme was developed, allowing parallel calculation and construction of optical density characteristics for different transformations, determining their deviations, sensitivity to parameter changes, and assessing the intensity of visual perception within the specified tone reproduction range. The results of simulation modeling in the form of optical density dependencies, their sensitivity, and intensity of visual perception for different transformation algorithms were presented and analyzed for their properties. It was established that the proposed exponential algorithm provides better image perception by the human visual system, which is its advantage.

Keywords

Modeling, decision-making, optical density, transformation, logarithmic algorithm, exponential algorithm, simulation, analysis, perception properties.

1. Introduction

Logarithmic and exponential transformation algorithms for optical density are used in image processing to enhance contrast and image quality. Both algorithms rely on fundamental mathematical principles and utilize the logarithmic and exponential functions, respectively.

The logarithmic transformation algorithm is based on the natural logarithmic function. The main idea is to compress high optical density values, reducing them, while expanding low density values, increasing them. This allows for a more detailed image with improved contrast.

The exponential transformation algorithm utilizes the exponential function to enhance image contrast. This algorithm increases the optical density value based on the input value, highlighting details where the optical density is low. Modeling the logarithmic and exponential transformation algorithms involves steps such as loading the image with optical density, computing the logarithmic or exponential transformation based on the selected algorithm, adjusting constants to achieve the desired level of contrast, and saving the modified image with improved contrast.

International Scientific Symposium «Intelligent Solutions» IntSol-2023, September 27–28, 2023, Kyiv-Uzhhorod, Ukraine
EMAIL: durnyak@uad.lviv.ua (Bohdan Durnyak); lutolen@i.ua (Mikola Lutskiv); pshepita@gmail.com (Petro Shepita); polishchukinn@gmail.com (Inna Polishchuk);
ORCID: 0000-0003-1526-9005 (Bohdan Durnyak); 0000-0002-2921-3662 (Mikola Lutskiv); 0000-0001-8134-8014 (Petro Shepita); 0009-0002-6395-4744 (Inna Polishchuk);

By using modeling techniques for these algorithms, one can investigate their impact on image quality and find optimal constant values for different types of images and scenarios.

1.1. Problem Statement

In the historical evolution of photographic processes and images, the attenuation of light flux began to be defined, and the reflection (or transmission) of light flux was quantified using the reflection coefficient. To quantitatively evaluate the light attenuation characteristics of an object, the decimal logarithm of opacity, known as optical density, was introduced. Later, this method was applied in printing to determine the darkness level of images on prints based on the light reflection from the image surface (scales), and the assessment was performed using optical density as the decimal logarithm of the reflection coefficient [1, 3, 7, 9-16]. However, certain sources [7, 8, 9, 22, 25] point out its drawbacks, such as significant errors in measuring small and large optical densities and the inconsistency of the logarithmic algorithm in relation to the human visual system's perception of optical density. Nevertheless, there is a lack of sufficient evidence and analysis regarding this expression and its characteristics. Therefore, modeling the logarithmic and exponential transformation algorithms for optical density is an important task.

1.2. Analysis of recent research and publications

Densitometers are devices designed to measure the intensity of reflected or transmitted light. They are used to determine optical density, relative area of printing elements, contrast, and other parameters. According to the international standard ISO5-2, the optical density of inked areas on a print (scales) is determined based on the reflection coefficient and quantitatively assessed using the optical density of reflection, which is the decimal logarithm of the inverse of the reflection coefficient [4,5,7, 17]. If the entire light flux is reflected from the image (patch), its tenths, hundredths, or thousandths are represented by optical densities of 0.1, 0.2, 0.3, respectively. The reflection coefficient depends on the degree of light absorption, the thickness of the ink layer and substrate, and a portion is reflected onto the densitometer receiver, which quantitatively evaluates individual parameters.

In [7, 18], the challenges of determining specific parameters through densitometric methods are discussed: large errors in measuring small optical densities, significant errors in estimating the areas of halftone elements in mid-tones up to 20%, and determination of photoform tone in mid and light tones in certain densitometers with errors of 10-20%. Optical density does not always correspond adequately to human visual perception of tonal gradations and does not reflect human tonality perception. In the presented and other publications, there is a lack of connection between visual perception and optical density of halftone images, which prevents establishing the relationship between the visual system and the optical density of printed images [8, 20].

The author's work [6] addresses the task of modeling the intensity of visual perception of the optical density of a halftone image. The results of simulation modeling are presented in the form of the dependence of visual perception intensity on optical density within a given tonal transmission interval, and its properties are analyzed. It is established that the human visual system poorly perceives and distinguishes image details in the dark tonal interval. In the light tonal transmission interval of $0 \leq D \leq 0.3$, the visual perception curves exhibit higher intensity, indicating better perception of image details. The goal of the article is to develop a model for the logarithmic and exponential transformation algorithms for optical density, determine and construct their characteristics, establish the relationship between the intensity of visual perception and the optical density of grayscale images, and analyze their properties.

2. Presentation of the main research material

Optical measurements are used in the field of printing for controlling originals, printing plates, printed impressions, and more. For this purpose, densitometers (density - the ability of an object to absorb light) are used, which are devices designed to measure the intensity of transmitted or reflected

light. They are used to determine optical density, relative area of printing elements, thickness of ink layers, image contrast, and more [1, 7,19, 21]. The optical density of darkened (printed) areas on the original (impression) is quantitatively assessed based on the optical density of reflection. According to ISO standard 5-2, optical density of reflection is determined by the decimal logarithm of the reciprocal of the reflection coefficient [7, 23-28].

$$D_0 = l_g \frac{1}{R_0} \; if \; 0 \le R_0 \le 1, \tag{1}$$

The reflection coefficient R_0 is the ratio of the reflected light flux F_p from the object under measurement to the intensity of the incident flux F_0 that falls onto the object under measurement.

$$R_0 = \frac{F_p}{F_0}, \tag{2}$$

If the entire light flux is reflected from the image (target), its tenth, hundredth, or thousandth part, then the optical density will be 0, 1, 2, 3. Substituting the coefficient (2) into equation (1), we obtain an expression for determining the reflected optical density.

$$D_0 = l_g \frac{F_0}{F_p}, \tag{3}$$

Expression (1) represents a mathematical logarithmic algorithm for determining the reflected optical density, while expression (3) represents an algorithm for the hardware implementation of a device to determine optical density and its modeling. Since the logarithmic algorithm for determining optical density has several drawbacks mentioned above, an alternative exponential algorithm for determining reflected optical density is proposed.

$$D_e = D_n(exp(-bR_0)), if \; 0 \le R_0 \le 1, \tag{4}$$

D_n - nominal value of optical density,

b - coefficient that determines the shape of the curve and is chosen within the range ($6 \le b \le 9$).

Based on the above, structural schemes of optical density models have been developed using the MATLAB Simulink package, which allow for parallel computation of reflected optical density using the logarithmic algorithm (3) and the exponential algorithm (4) and are depicted in Figure 1.

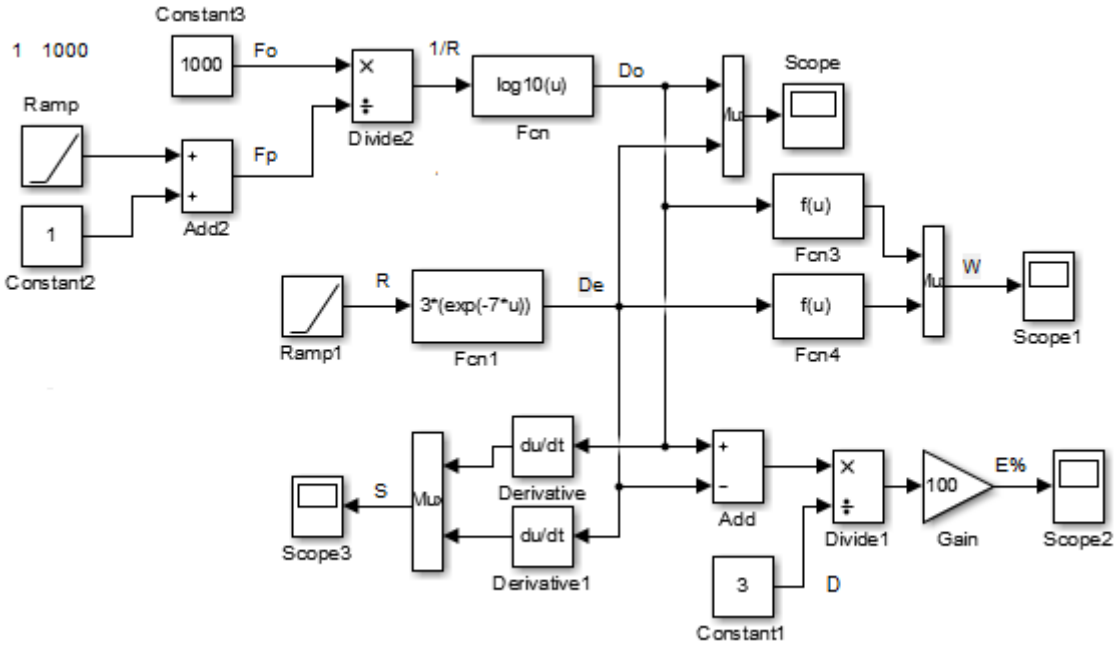

Figure 1: Structural diagrams of optical density models with logarithmic and exponential algorithms

For increased accuracy and convenience, a falling light flux F_0=1000 is set using the Constant block. The Ramp block generates the reflected light flux F_{p+1} (with an added unit to shift the logarithmic characteristic to zero), which is fed into the second input of the division block. As a result, the reflection coefficient is obtained at the output, which is then passed to the Math Function

block Fcn. The dialog window of Fcn contains the program (expression) for calculating the reflection optical density D_0 using the logarithmic algorithm. The second Ramp block generates the reflection coefficient within the range $0 \leq R_0 \leq 1$ and is fed into the second Math Function block Fcn1, which contains the program (expression 4) for determining the optical density De using the exponential algorithm. The calculation results of the optical densities are visualized using the Scope block. To compare the results obtained by different algorithms, the deviations of the optical densities are determined.

$$E = \frac{D_0 - D_e}{D_n} 100\%, \tag{5}$$

The addition and division operations, located at the bottom of the diagram, implement it.

The model parameters were set for the nominal optical density D_n = 3.0, b = 7, and other parameters are directly provided in Figure 1. The simulation results of the optical densities calculated using different algorithms are depicted in Figure 2.

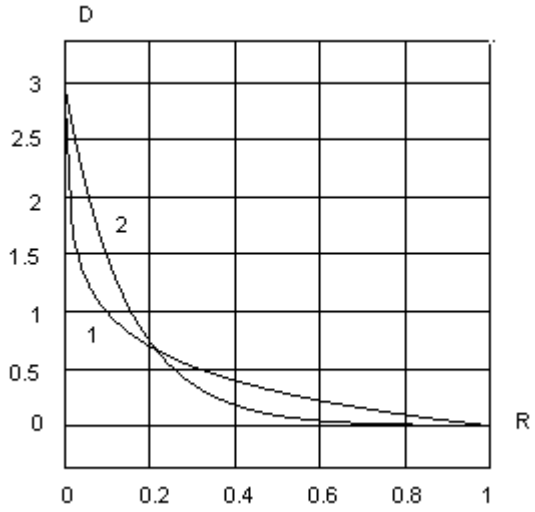

Figure 2: The reflection optical densities determined using different algorithms.

The characteristic of optical density 1, determined using the logarithmic algorithm, is a logarithmic curve with a steep slope. In the initial range, the optical density sharply decreases from D_m = 3.0 to D_0= 0.85 at R_0 = 0.15, and then gradually decreases, almost linearly, towards zero. On the other hand, the characteristic of optical density 2, determined using the potential algorithm, has a significantly smaller slope at the beginning of the range and gradually approaches zero. It should be noted that the characteristics are practically indistinguishable in the highlight tones. For comparison, the deviations of optical densities determined using different algorithms are shown in Figure 3.

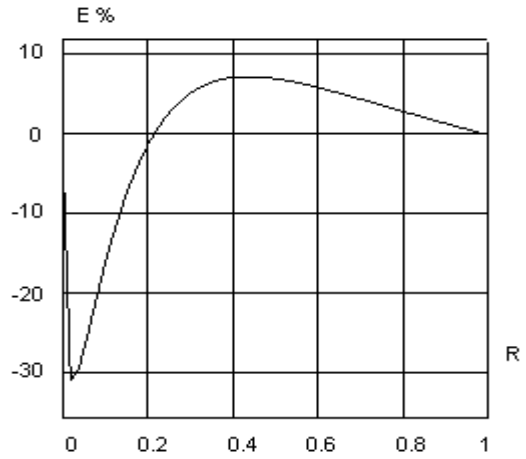

Figure 3: Deviations of optical densities determined using different algorithms.

The maximum deviation of optical density occurs at the beginning of the range and amounts to -27.5%. It gradually decreases and crosses zero at a coefficient of $R_0 = 0.12$, becoming positive with a maximum deviation of +10% and gradually approaching zero. Therefore, the main deviation of optical densities occurs only at the beginning of the range with the maximum density value.

As mentioned earlier, there are problems in determining individual parameters using densitometric methods, and significant errors in their determination exist. One of the reasons for these errors is the sensitivity of the algorithms to the reflection coefficient R0, especially at low values. It is proposed to determine the sensitivity of the algorithms to changes in optical density using derivatives.

$$S = \frac{dD}{dR_0}, \tag{6}$$

To determine the sensitivity in the model, Derivative blocks were used, which are located at the bottom of the diagram. As an example, the sensitivity of the optical density algorithms for small values of reflection coefficients was determined, as shown in Figure 4 in close-up.

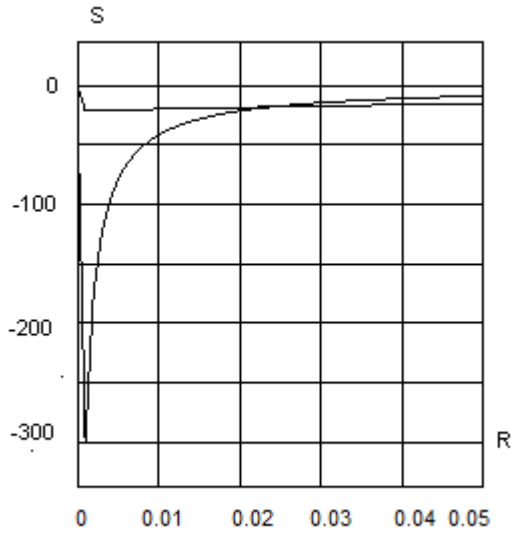

Figure 4: Graphical dependence of the sensitivity of optical densities for different algorithms.

At nominal values of optical density D=3.0 for the logarithmic algorithm of optical density, the maximum sensitivity value is S_m=-300, gradually decreasing. At a coefficient R_0=0.02, the sensitivity of optical density leads to significant errors in determining individual parameters using densitometric methods. On the other hand, the sensitivity of the exponential algorithm is practically constant and close to -25-30. Therefore, in terms of sensitivity, the proposed exponential algorithm significantly outperforms the logarithmic one.

As mentioned above, optical density does not always correspond to visual perception based on Weber-Fechner's law, which describes the human visual system's perception of light. Since the reproduction of images by printing methods is done using black ink, which is predominantly described by optical density, it does not directly take into account the properties of the human visual system. Later, it was established that Weber-Fechner's law, which is psychophysical and describes the perception of physical quantities by sensory organs, is valid, for example, for the human perception of sound volume, light intensity, mechanical force. In other words, sensation is proportional to the logarithm of the stimulus intensity [2, 4, 8, 27, 30, 36]. Since Weber-Fechner's law is psychophysical and describes the perception of physical quantities by sensory organs, it is logical to assume that it is valid for the perception of optical density, which the human visual system can distinguish on an elementary monochromatic image plane. Based on the above, by analogy with Weber-Fechner's law, a model of visual perception intensity of optical density can be formulated [6, 14, 31, 32, 34].

$$W = C - n \lg\left(\frac{D_n}{D_0} + 1\right) \tag{7}$$

where D_n – the nominal value of optical density, D_0 – the threshold of optical density discrimination, n is the number of discrimination thresholds, 1 is introduced for initial offset, and C – an integration

constant dependent on initial conditions [4, 15, 33, 35]. The models of visual perception intensity (7) are implemented using mathematical function blocks Fcn3 and Fcn4 for different algorithms of optical density. We set the maximum value of optical density Dn=3.0, Do=0.7, and chose the number of discrimination thresholds n=24, and integration constant C=38. The results of simulation modeling of intensity perception characteristics for different algorithms of optical density are shown in Figure 5.

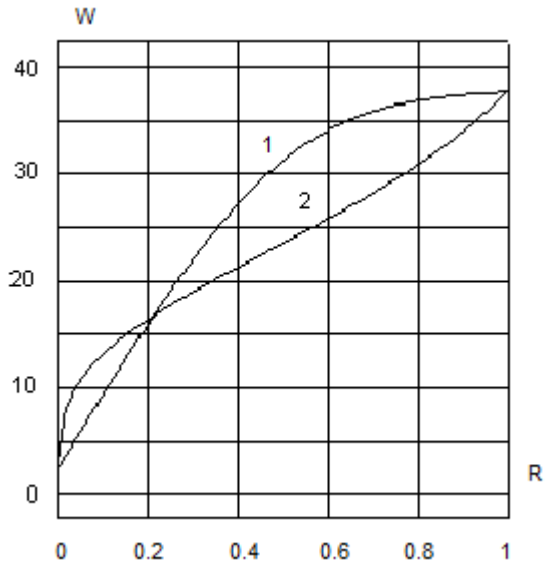

Figure 5: Characteristics of visual perception intensity for different algorithms of optical density.

The characteristic of visual perception 2 for the logarithmic algorithm of optical density determination at the beginning of the range $\leq R_0 \leq 0.2$ ($0 \leq W \leq 14.5$) follows Weber-Fechner's law of optical density perception. However, after that, the characteristic is nearly linear and converges to a final value of W = 38. Overall, the intensity characteristic of visual perception determined by the logarithmic algorithm does not comply with Weber-Fechner's law. On the other hand, the characteristic 1 of visual perception for the exponential algorithm of optical density determination follows Weber-Fechner's law throughout the entire tonal range.

Since densitometry is widely used for control and determination of various parameters in the preparation stage of image printing, plate production, and printing processes, involving various scales, understanding the peculiarities of human vision and the provided models and algorithms for transforming optical density and intensity characteristics of visual perception will contribute to enhancing the efficiency of monitoring individual stages and image quality.

3. Conclusions

A model of traditional logarithmic and exponential algorithms has been developed to determine the optical density of monochrome halftone images within a specified density range in offset printing. The algorithms are presented in mathematical expressions as hardware implementation algorithms for a measuring device. The sensitivity of the algorithms to changes in optical density is determined using derivatives. An extension of Weber-Fechner's law, which describes the perception of various physical quantities by human sensory organs and is proportional to the logarithm of stimulus intensity, is applied to perceive optical density by the human visual system. A model of visual perception intensity for optical density is proposed, enabling the determination and construction of perception characteristics for different algorithms of optical density determination.

Structural diagrams of optical density models in MATLAB: Simulink have been processed, allowing for parallel computation of reflection optical density using logarithmic and exponential algorithms. The deviations and the dependence of optical density sensitivity, leading to significant errors in determining individual parameters using densitometric methods, are determined. The results of simulation modeling indicate that the characteristic of optical density determined by the

logarithmic algorithm has a steep slope in the shadows, while the characteristic determined by the exponential algorithm has a significantly gentler slope, resulting in a maximum deviation of 27.5%. The maximum sensitivity value of optical density is determined as Sm = -300, leading to significant errors in determining individual parameters using densitometric methods. However, the sensitivity of the exponential algorithm is practically constant and close to 25...30. The characteristic of intensity perception determined by the logarithmic algorithm does not comply with Weber-Fechner's law. In contrast, the characteristic of perception for the exponential algorithm complies with Weber-Fechner's law throughout the entire tonal range.

4. References

[1] J. Felici, Complete Manual of Typography: A Guide to Setting Perfect Type. Pearson Education, Limited, 2018.

[2] U. A. Nnolim, "An adaptive RGB colour enhancement formulation for logarithmic image processing-based algorithms", Optik, v. 154, p. 192–215, 2018. doi.org/10.1016/j.ijleo.2017.09.102.

[3] N. Karmaker, "Digital Image Processing and Its Application for Medical Physics and Biomedical Engineering Area", Digital Image Processing Applications. IntechOpen, 2022. doi.org/10.5772/intechopen.100619.

[4] V. A. Samogorov and E. D. Konkina, "Johannes Itten: The Seven Color Contrasts", Urban construction architecture, v. 11, № 3, p. 97–103, 2021. doi.org/10.17673/vestnik.2021.03.14.

[5] "33rd International Conference on Digital Printing Technologies (NIP)", NIP & Digit. Fabr. Conf., v. 33, № 1, с. i—xliv, 2017. doi.org/10.2352/issn.2169-4451.2017.33.1.

[6] V. Lakshminarayanan, "Maxwell, color vision, and the color triangle", у *Light Nature VII*, J. A. Shaw, K. Creath та V. Lakshminarayanan, Ред. San Diego, United States, 2019. SPIE, 2019. doi.org/10.1117/12.2529364

[7] "METROLOGY, STANDARDIZATION, QUALITY: THEORY AND PRACTICE (MSQ-2017)", *J. Physics: Conf. Ser.*, v. 998, p. 011001, 2018. doi.org/10.1088/1742-6596/998/1/011001

[8] Y. Li, H. Jiang, L. Yu та J. Li, "High-Precision Time Delay Estimation Based on Closed-Form Offset Compensation", *Comput. Model. Eng. & Sci.*, v. 134, № 3, p. 2123–2136, 2023. doi.org/10.32604/cmes.2022.021407

[9] Imamović, B., Halilčević, S.S. and Georgilakis, P.S. (2022) “Comprehensive fuzzy logic coefficient of performance of absorption cooling system,” Expert Systems with Applications, 190, p. 116185. Available at: https://doi.org/10.1016/j.eswa.2021.116185.

[10] Salem, A.A., ElDesouky, A.A. and Alaboudy, A.H. (2022) “New Analytical Assessment for fast and complete pre-fault restoration of grid-connected fswts with fuzzy-logic pitch-Angle Controller,” International Journal of Electrical Power & Energy Systems, 136, p. 107745. Available at: https://doi.org/10.1016/j.ijepes.2021.107745.

[11] “Fuzzy relations” (2018) A First Course in Fuzzy Logic, pp. 225–252. Available at: https://doi.org/10.1201/9780429505546-12.

[12] “Complex fuzzy sets and complex fuzzy logic. an overview of theory and applications” (2018) Fuzzy Logic Theory and Applications, pp. 309–325. Available at: https://doi.org/10.1142/9789813238183_0011.

[13] Rahmah, F., Hidayanti, F., Wati, E. K., Lestari, K. R., & Sudrajat, S. W. “Solar Panel Motor tracker model comparison between PID and Fuzzy PD” (2022) International Journal of Renewable Energy Research [Preprint], (Vol12i3). Available at: https://doi.org/10.20508/ijrer.v12i3.13117.g8525.

[14] S. Aslam, Y.-C. Chak, M. H. Jaffery, and R. Varatharajoo, “The Fuzzy PD control for combined energy and Attitude Control System,” Aircraft Engineering and Aerospace Technology, vol. 94, no. 10, pp. 1806–1824, 2022.

[15] S. Raja and N. P. Ananthamoorthy, “Evaluation of newly developed liquid level process with PD and PID controller without altering material characteristics,” Journal of New Materials for Electrochemical Systems, vol. 24, no. 3, pp. 218–223, 2021.

[16] E. Ontiveros-Robles, P. Melin, and O. Castillo, “Comparative analysis of noise robustness of type 2 fuzzy logic controllers,” Kybernetika, pp. 175–201, 2018.

[17] J. Yoo, D. Lee, C. Son, S. Jung, B. I. Yoo, C. Choi, J.-J. Han, and B. Han, “Rascanet: Learning tiny models by raster-scanning images,” 2021 IEEE/CVF Conference on Computer Vision and Pattern Recognition (CVPR), 2021.
[18] E. Alzaghoul, M. B. Al-Zoubi, R. Obiedat, and F. Alzaghoul, “Applying machine learning to DEM raster images,” Technologies, vol. 9, no. 4, p. 87, 2021.
[19] L. Zweifel, M. Samarin, K. Meusburger, V. Roth, and C. Alewell, “Identification of soil erosion in alpine grasslands on high-resolution aerial images: Switching from object-based image analysis to deep learning,” 2020.
[20] Durnyak, B., Lutskiv, M., Shepita, P., Sheketa, V., Karpyn, R., & Pasyeka, N. (2022). *Analysis of transfer of modulated ink flows in a short printing system of parallel structure* doi:10.1007/978-3-031-04812-8_2
[21] Durnyak, B., Lutskiv, M., Shepita, P., Karpyn, R., Sheketa, V., & Pasieka, M. (2022). *Modelling of tone reproduction with round raster elements in a short printing system of parallel structure* doi:10.1007/978-3-031-04812-8_4
[22] Durnyak, B., Lutskiv, M., Shepita, P., Hunko, D., & Savina, N. (2021). Formation of linear characteristic of normalized raster transformation for rhombic elements. Paper presented at the *CEUR Workshop Proceedings, , 2853* 127-133
[23] Durnyak, B., Lutskiv, M., Shepita, P., Hunko, D., & Savina, N. (2021). Formation of linear characteristic of normalized raster transformation for rhombic elements. Paper presented at the CEUR Workshop Proceedings, 2853, 127-133.
[24] L. Kakinada and K. Singh, “WCA optimized fuzzy PD controller for stabilizing the two wheel self-balancing robot,” 2021 Asian Conference on Innovation in Technology (ASIANCON), 2021., doi:10.1109/ASIANCON51346.2021.9544711
[25] L. Zweifel, M. Samarin, K. Meusburger, V. Roth, and C. Alewell, “Identification of soil erosion in alpine grasslands on high-resolution aerial images: Switching from object-based image analysis to deep learning,” 2020.
[26] M. Azimipour, R. J. Zawadzki, I. Gorczynska, J. Migacz, J. S. Werner, and R. S. Jonnal, “Intraframe motion correction for Raster-scanned adaptive optics images using strip-based cross-correlation lag biases,” PLOS ONE, vol. 13, no. 10, 2018.
[27] Z. Mingsong, J. Lingwen, and L. Shuxiao, “A transformation of the CVIS method to eliminate the irregular frequency,” Engineering Analysis with Boundary Elements, vol. 91, pp. 7–13, 2018.
[28] J. Harder, “Looking at other Adobe applications for GIF Animation Creation and GIF alternatives,” Creating GIF Animations, 2022.
[29] Friedrich, L., Begley, M. Printing direction dependent microstructures in direct ink writing. Additive Manufacturing, Vol. 34, P. 2020101192.
[30] Jurečić, D., Žiljak, V., Gršić, J. Ž., Rajković, I. Near infrared spectrography of colorants for offset printing with individualized rasters on drug packaging. Acta Graphica, Vol. 29(4), 2020, PP. 7-12.
[31] Kusaka, Y., Fukuda, N., Ushijima, H. Recent advances in reverse offset printing: an emerging process for high-resolution printed electronics.
[32] T. V. Neroda, L. V. Slipchyshyn та I. O. Muzyka, “Adaptive toolkit of branch-oriented workshop environment for enlargement the cloud-based e-learning media platform”, CTE Workshop Proc., vol. 8, p. 423–437 doi.org/10.55056/cte.298.
[33] Kusaka, Y., Kanazawa, S., & Ushijima, H. Design rules for vertical interconnections by reverse offset printing. Journal of Micromechanics and Microengineering, Vol. 28(3), 2018, P. 035003.
[34] Litunov, S. N., Gusak, E. N., Toshhakova, Y. D. Numerical study of printing ink structuring. In Journal of Physics: Conference Series. Vol.1050(1), 2018, P. 012045
[35] Moreira, A., Silva, F. J. G., Correia, A. I., Pereira, T., Ferreira, L. P., De Almeida, F. Cost reduction and quality improvements in the printing industry. Procedia manufacturing, Vol. 17, 2018, PP. 623-630.
[36] Nikolov, A., Murad, S., Wasan, D., Wu, P. How the capillarity and ink-air flow govern the performance of a fountain pen. Journal of colloid and interface science, Vol. 578, 2020, PP.660-667.